Metal Clusters

DOI: 10.1002/anie.201301982

Ion Exchange of Protons by Coinage Metals to Give Gold and Silver Encapsulation within a Pseudo-D_{2d} Distorted Face-Capped Pd_{14} Cubic Kernel: $[(\mu_{14}\text{-}M)Pd_{22}(CO)_{20}(PEt_3)_8]^+$ (M = Au, Ag)**

Evgueni G. Mednikov and Lawrence F. Dahl**

Dedicated to Professor Mike Mingos

During the last 10–15 years, bimetallic gold–palladium nanosized clusters have attracted considerable attention owing to their greater stabilities[1a] and enhanced catalytic performances compared to their single-metal counterparts.[1b,c] Likewise, a recent report[1d] revealed that bimetallic Ag-Pd nanoparticles had higher catalytic activity and selectivity for oxidation of propene to propene oxide with molecular oxygen (in methanol) than did Pd salts and Pd and Ag monometallic nanoparticles. However, syntheses of stoichiometrically defined nanosized bimetallic palladium composites with Group 11 coinage-metal elements still remain challenging:[2a] there have been no previous publications of nanosized Ag-Pd clusters.[2b] Recently we reported the synthesis of the bicuboctahedral Au-Pd $Au_2Pd_{28}(CO)_{26}(PEt_3)_{10}$,[2c] which, unlike its structurally analogous non-isovalent homopalladium Pd_{30} cluster, was obtained under CO atmosphere by reactions of coordinatively unsaturated $Pd_n(CO)_x(PR_3)_y$ species (resulting from CO-induced fragmentations of either of two structurally dissimilar homopalladium Pd_n clusters, $n = 23$, 38) with the CO-tolerant Au-centered cuboctahedral cluster precursor, $Au_2Pd_{21}(CO)_{20}(PEt_3)_{10}$. Based upon both direct crystallographic evidence and DFT calculations,[2c] the higher stability to CO of the Au_2Pd_{28} cluster was attributed to electron delocalization of each Au 6s valence electron for the two adjacent interior Au atoms instead of the formation of a localized electron-pair Au–Au bond. This important stereochemical implication has particular relevance to the recent report[1e] that the presence of Au in Au-Pd nanoparticle catalysts, used for the complete conversion of formic acid into high-purity hydrogen (and CO_2) for chemical hydrogen storage, suppresses CO poisoning, in sharp contrast to early deactivation of the corresponding Pd counterpart material by carbon monoxide.

Herein we present a different synthetic approach to obtain a gold-encapsulated nanosized Au-Pd cluster; application of this method is also shown to provide preparation of the first corresponding high-nuclearity Ag-Pd cluster. The resulting two remarkable isostructural nanosized M-centered cluster monocations, $[(\mu_{14}\text{-}M)Pd_{22}(CO)_{20}(PEt_3)_8]^+$, M = Au (**1**), Ag (**2**), with $[(CF_3CO_2)_2H]^-$ counterions, were obtained by two-step/one-pot reactions of $Pd_{10}(CO)_{12}(PEt_3)_6$ with CF_3CO_2H (in acetone at 50 °C) followed by coinage-metal ion exchange of protons by the addition of either $Au(SMe_2)Cl$ (45–60 % yields) or $Ag(CF_3SO_3)$ (28 % yield), respectively. A similar attempt to isolate the Cu-Pd analogue by incorporation of Cu^+ metal ion was unsuccessful. This preparative method outlined in the reaction sequence (1) is based upon: a) prior treatment of the homopalladium precursor, $Pd_{10}(CO)_{12}(PEt_3)_6$ (**4**), with CF_3CO_2H acid in the presence of Me_3NO that affords a non-isolated protonated species (for example, monoprotonated $[HPd_n(CO)_x(PEt_3)_y]^+$ with a $[CF_3CO_2]^-$ counterion); and b) addition of either $Au(SMe_2)Cl$ or $Ag(CF_3SO_3)$ which, by ion exchange of proton(s) by a coinage metal, gives rise to formation of the resulting $[(\mu_{14}\text{-}M)Pd_{22}(CO)_{20}(PEt_3)_8]^+$ cluster cations that were isolated and crystallographically/spectroscopically characterized as $[(CF_3CO_2)_2H]^-$ salts (**1** and **2**) and as the $[PF_6]^-$ salt (**1a**) obtained through metathesis of the $[(CF_3CO_2)_2H]^-$ salt (**1**) with $[n\text{Bu}_4][PF_6]$.

$$Pd_{10}(CO)_{12}(PEt_3)_6\ (\mathbf{4}) \xrightarrow[\text{b) } Au(SMe_2)Cl \text{ or } Ag(CF_3SO_3),\ 50\,^\circ C,\ 2\,h]{\text{a) } CF_3CO_2H/Me_3NO,\ 50\,^\circ C,\ 30\,min} [MPd_{22}(CO)_{20}(PEt_3)_8][(CF_3CO_2)_2H],\ M = Au\ (\mathbf{1}),\ Ag\ (\mathbf{2}) \quad (1)$$

In these reactions, CF_3CO_2H (HX) plays several roles: a) in eliminating excess phosphine ligands as a phosphonium salt, $[HPEt_3]X$; b) in facilitating CO ligand oxidation (by Me_3NO) by formation of a quaternary salt, $[HNMe_3]X$; and c) in generating intermediate precursor(s), such as protonated $[HPd_n(CO)_x(PEt_3)_y]X$ species. The observation of a high-field signal at −17.5 in a ^1H NMR spectrum of the C_6D_6 extract from its evaporated residue points to the expected nature of this protonated species as a hydrido palladium complex.[3]

The crystal structures of $[(\mu_{14}\text{-Au})Pd_{22}(\mu_2\text{-CO})_{16}(\mu_3\text{-CO})_4(PEt_3)_8][(CF_3CO_2)_2H]$ (**1**), $[(\mu_{14}\text{-Au})Pd_{22}(\mu_2\text{-CO})_{16}(\mu_3\text{-CO})_4(PEt_3)_8][PF_6]\cdot 0.5\,Me_2CO$ (**1a**·0.5 Me_2CO), and $[(\mu_{14}\text{-Ag})Pd_{22}(\mu_2\text{-CO})_{16}(\mu_3\text{-CO})_4(PEt_3)_8][(CF_3CO_2)_2H]$ (**2**) were unambiguously established from low-temperature (100 K) CCD X-ray diffractometry studies. Of prime interest is that the isostructural cations of **1** and **1a** (M = Au) and **2** (M = Ag) are electronically equivalent (isovalent) and structurally analogous to the known neutral homopalladium species (μ_{14}-

[*] Dr. E. G. Mednikov, Prof. L. F. Dahl
Department of Chemistry University of Wisconsin-Madison
1101 University Ave. Madison, WI 53706 (USA)
E-mail: mednikov@chem.wisc.edu
dahl@chem.wisc.edu

[**] This research was supported by the University of Wisconsin-Madison. We thank Dr. Ilia Guzei (UW-Madison) for crystallographic advice.

Supporting information for this article is available on the WWW under http://dx.doi.org/10.1002/anie.201301982.

Pd)$Pd_{22}(CO)_{20}(PEt_3)_8$ (**3**) {M = Pd}.[4] Furthermore, **1** was also obtained from the latter cluster **3** (see below) by replacement of its centered encapsulated Pd atom with the isovalent Au^+. In **1** and **2**, the determined bis(trifluoroacetate) hydrogen counterion, $[(CF_3CO_2)_2H]^-$, which possesses an extremely short O···O distance of 2.4 Å with a modeled symmetrical hydrogen bond, is analogous to those previously reported.[5] Because the crystal structure of the $AuPd_{22}$ cluster (**1a**) with the $[PF_6]^-$ counterion was determined more precisely than that of **1** with the $[(CF_3CO_2)_2H]^-$ counterion, its geometrical parameters are used in comparison with those of **2** and **3**.

The metal frameworks of these two new heterometallic MPd_{22} clusters (**1** and **2**) and the neutral $PdPd_{22}$ cluster (**3**)[4] ideally conform to *pseudo-*D_{2d} symmetry. Figure 1 shows that the M-centered Ag or Au atom is likewise encapsulated within a geometrically deformed Pd_{14} cubic kernel composed of eight corner Pd(A) atoms and six face-capping Pd(B) and Pd(C) atoms. The Pd(A) atoms form alternating bonding $Pd(A_1)$–$Pd(A_1)$ and nonbonding $Pd(A_1)\cdots Pd(A_2)$ edges on the S_4-related top and bottom $Pd(A)_4$ faces and four σ_d-related weaker vertical bonding $Pd(A_1)$–$Pd(A_3)$ edges on the four side $Pd(A)_4$ faces; two Pd(C) and four Pd(B) atoms strongly cap the top/bottom and four side $Pd(A)_4$ faces, respectively. This M-centered MPd_{14} cubic kernel is additionally linked to four tetracapped $Pd(PEt_3)$ and four edge-bridged (wingtip) $Pd(PEt_3)$ fragments. Table S1 (Supporting Information) compares the mean distances and individual ranges under *pseudo-*D_{2d} symmetry for the $[(\mu_{14}\text{-Au})Pd_{22}(\mu_2\text{-CO})_{16}(\mu_3\text{-CO})_4(PEt_3)_8]^+$ cation (**1a**) (M = Au; $[PF_6]^-$ counterion) and $[(\mu_{14}\text{-Ag})Pd_{22}(\mu_2\text{-CO})_{16}(\mu_3\text{-CO})_4(PEt_3)_8]^+$ cation (**2**) (M = Ag; $[(CF_3CO_2)_2H]^-$ counterion) with those for the known neutral species $[(\mu_{14}\text{-Pd})Pd_{22}(CO)_{20}(PEt_3)_8]$ (**3**) {M = Pd}.

Although the metal-core architecture in **3** is closely similar to those of the isostructural monocations in **1**, **1a**, and **2**, the much poorer precision of the light-atom molecular parameters in the previously determined crystal structure of **3**[4] is apparent from the markedly wider, unrealistic ranges of the individual C–O bond lengths in **3** given in Table S1 (Supporting Information) compared to reasonable values found in **1**, **1a**, and **2**. Consequently, the Figure 2 caption excludes the less meaningful metal–ligand mean distances in **3** in providing metal–ligand mean distances only for **1a** and **2**.

Figure 1 and Table S1 (Supporting Information) show that corresponding mean M–Pd and Pd–Pd distances in the MPd_{22} metal cores in both the encapsulated gold and silver cations of **1a** and **2**, respectively, are either identical or very close (within 0.01–0.02 Å) but substantially different from those in the neutral $PdPd_{22}$ metal core (**3**). First, the identical mean bonding M–Pd(A) connectivities in **1a** (M = Au) and **2** (M = Ag) are 0.03 Å shorter than that for the mean homopalladium Pd–Pd(A) connectivity in **3** (M = Pd), whereas the mean bonding connectivities from the encapsulated heteroatoms M = Au in **1a** and M = Ag in **2** to the six face-capping atoms are longer to Pd(B) by 0.12 Å in **1a**/0.10 Å in **2** and to Pd(C) by 0.03 Å in **1a**/0.05 Å in **2**. In turn, these variations of mean M–Pd_{14} connectivities in **1a** and **2** versus those in **3** give rise to less-distorted top and bottom $Pd(A)_4$ faces with alternating mean bonding/nonbonding Pd(A)–Pd(A) edges of 2.85 Å/3.96 Å in **1a** and 2.85 Å/3.95 Å in **2** versus 2.81 Å/4.06 Å in **3**; the mean distances for the four weaker bonding vertical Pd(A)–Pd(A) edges of the four equivalent side $Pd(A)_4$ faces are similar for **1a** (3.17 Å), **2** (3.19 Å), and **3** (3.22 Å). Despite this redistribution of mean distances for the MPd_{14} cubic kernel in **3** compared to those in **1a** and **2**, the mean for the 14 individual distances from the encapsulated M atom to the D_{2d}-distorted face-centered Pd_{14} cube is virtually identical in **1a** (2.94 Å), **2** (2.93 Å), and **3** (2.92 Å).

Figure 2 shows the steric dispositions of the eight PEt_3 and 20 bridging CO groups in **1a**, which are closely related to

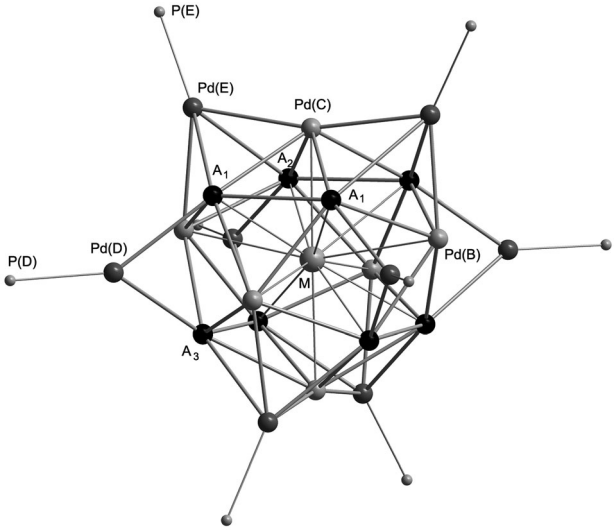

Figure 1. Metal-core $[(\mu_{14}\text{-M})Pd_{22}P_8]$ geometry of *pseudo-*D_{2d} symmetry in electronically equivalent (isovalent) **1** (M = Au; $[(CF_3CO_2)_2H]^-$ counterion), **1a** (M = Au; $[PF_6]^-$ counterion), **2** (M = Ag; $[(CF_3CO_2)_2H]^-$ counterion), and neutral **3** (M = Pd). The centered M atom is encapsulated within the D_{2d}-deformed cube of Pd(A) atoms (black) that is face-capped by two vertical Pd(C) atoms and four horizontal Pd(B) atoms. This resulting face-capped MPd_{14} cubic kernel is additionally coordinated to four tetracapped Pd(E)–P(E) fragments and to four edge-bridging (wingtip) Pd(D)–P(D) fragments. The improper S_4 axis passes through the centered M and both face-capping Pd(C) atoms, and each horizontal C_2 axis passes through the M and two of the four wingtip Pd(D) atoms. Each of the two symmetry-equivalent vertical σ_d mirror planes that bisect the pair of horizontal C_2 axes passes through M, both Pd(C), two of the four horizontal face-capping Pd(B) atoms, and two adjacent Pd(E) atoms. For the isostructural metal-core geometries of **1** and **1a** (M = Au), **2** (M = Ag), and **3** (M = Pd), mean distances [Å] are given for **1a** followed by corresponding mean distances (in parentheses) for **2** and **3**, respectively. Bonding connectivities from the centered M atom: 2.88 (2.88; 2.91) to eight Pd(A), 2.85 (2.87; 2.82) to two Pd(C), and 3.09 (3.07; 2.97) to four Pd(B). The S_4-related top and bottom $Pd(A)_4$ faces each consist of alternating bonding and nonbonding Pd(A)–Pd(A) edges: 2.85 (2.85; 2.81) and 3.96 (3.95; 4.06), respectively; the four twofold-related $Pd(A)_4$ side faces are comprised of four weakly bonding Pd(A)–Pd(A) edges: 3.17 (3.19; 3.22). The two face-capping Pd(C) and four face-capping Pd(B) atoms are strongly coordinated to the Pd(A) cube: 8 Pd(C)–Pd(A) 2.77 (2.77; 2.78) and 16 Pd(B)–Pd(A) 2.74 (2.73; 2.71). Linkages of the M-centered face-capped MPd_{14} cubic kernel to four tetracapped Pd(*E*)–P(E) fragments and four edge-bridging (wingtip) Pd(D)–P(D) fragments: 8 Pd(*E*)–Pd(A), 2.92 (2.91;3.00), 4 Pd(*E*)–Pd(B) 2.69 (2.71; 2.68), 4 Pd(E)–Pd(C) 2.78 (2.78; 2.80), 8 Pd(D)–Pd(A) 2.71 (2.72; 2.72).

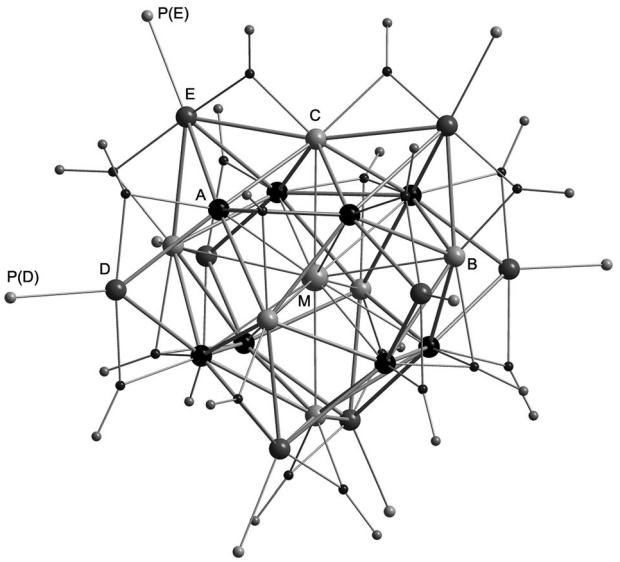

Figure 2. Overall metal-ligand geometry (without P-attached Et substituents) of the $[(\mu_{14}\text{-M})Pd_{22}(\mu_2\text{-CO})_{16}(\mu_3\text{-CO})_4(PEt_3)_8]^+$ cation in **1a** {M = Au; $[PF_6]^-$ counterion} that is essentially isostructural with the metal–ligand geometries of the cations in **1** (M = Au; $[(CF_3CO_2)_2H]^-$) and **2** (M = Ag; $[(CF_3CO_2)_2H]^-$). The orientation of the metal-core geometry and atom designations are the same as in Figure 1. The spacial distribution of the 8 P atoms and 20 bridging carbonyl ligands (consisting of four coordinated triply bridging and 16 doubly bridging CO groups) approximately conforms to D_{2d} symmetry. Mean metal–ligand distances [Å] under *pseudo-*D_{2d} symmetry for the isostructural **1a** (M = Au) and **2** (M = Ag; in parentheses): 4 Pd(D)–P(D) 2.30 (2.31), 4 Pd(E)–P(E) 2.33 (2.34), 8 Pd(A)–(μ_3-CO) 2.02 (2.01), 4 Pd(B)–(μ_3-CO) 2.29 (2.33); mean distances for the 32 Pd-(μ_2-CO) 2.03 (2.03), 16 (μ_2-C-O) 1.16 (1.15), 4 (μ_3-C-O) 1.17 (1.17).

those in **1** and **2** and roughly related to those in the less-precisely determined **3**. Four P(E) atoms are coordinated to the four tetracapped Pd(E) atoms and four P(D) atoms to the four wingtip Pd(D) atoms. The 16 doubly bridging CO groups link all eight bonding Pd(C)–Pd(E) and Pd(B)–Pd(E) edges of the tetracapped Pd(E) atoms and all eight bonding Pd(A)–Pd(D) edges of the wingtip Pd(D) atoms. The remaining four triply bridging COs asymmetrically cap triangular $Pd(A)_2Pd(B)$ faces of the Pd_{14} cubic kernel. Inclusion of the CO ligands in **1a**, **1**, and **2** ideally preserves D_{2d} symmetry.

In light of the proton being isolobal with $M = Ag^+$, Au^+, it is reasonable to observe its formal exchange by these coinage metal ions. In fact, this direct isolobal H^+/Au^+ relationship provides a prime illustration in support of the recently suggested modification by Raubenheimer and Schmidbaur[6f] of the initially proposed isolobal H^+/LAu^+ analogy.[6,7] Of prime significance is the resulting encapsulation[8] of the Group 11 metal ion within **1** and **2** regardless of the nature of the preformed protonated palladium species.[3] In complete contrast, for the vast majority of reactions of transition-metal compounds with coinage-metal salts, either peripheral attachment of a $[LM]^+$ fragment to one or more transition metals[9] or M-centered sandwich formation[10] occurs. A particular example of the former reaction is the electrophilic substitution of LAu^+ ($L = PPh_3$) for H^+ at the triplatinum center of $[Pt_3(\mu_3\text{-H})(\mu_2\text{-dppm})_3]^+$ ($dppm = Ph_2PCH_2PPh_2$) that gave rise to Pt_3Au $[Pt_3(\mu_3\text{-AuL})(\mu_2\text{-dppm})_3]^+$ and Pt_3Au_2 $[Pt_3(\mu_3\text{-AuL})_2(\mu_2\text{-dppm})_3]^{2+}$ clusters along with isolation of the intermediate $[Pt_3(\mu_3\text{-H})(\mu_3\text{-AuL})(\mu_2\text{-dppm})_3]^{2+}$.[11]

Although no protonated ionic palladium species were isolated, its formation after the first-step of the reaction of the $Pd_{10}(CO)_{12}(PEt_3)_6$ (**4**) precursor with CF_3CO_2H is apparent from the sharp increase in solubility in acetone used as the solvent. In fact, the solubility of the PEt_3-containig Pd_{10} precursor **4** as such in acetone is low, and furthermore all known neutral PEt_3-ligated clusters $Pd_n(CO)_x(PEt_3)_y$ of higher nuclearity, $n > 10$, are insoluble in this polar solvent. For the in situ generation of protonated species in acetone an elevated temperature (50 °C) is needed.[12] Small complexes with hydrido-like Pd-H connectivities are known, but most of them (in contrast to corresponding Ni and Pt complexes) are much less stable[13] and in many cases cannot be prepared by reactions analogous to those used for Ni and Pt.[13b] Thus, a cationic palladium hydride complex, $[PdHL_3]^+$, $L = PPh_3$, was observed in situ in equilibrium conditions upon protonation of PdL_4 at 25 °C with aqueous CF_3CO_2H (30 % H_2O) and likewise upon interaction of H_2 with $PdL_2(CF_3CO_2)_2$ at 70 °C in aqueous CF_3CO_2H in the presence of excess L.[14] The isolated and spectroscopically characterized unstable cationic platinum hydrido cluster, $[Pt_3H(CO)_3(PCy_3)_3]^+$, was obtained by protonation of the $[Pt_3(CO)_3(PCy_3)_3]$ cluster (in C_6H_6) with 54 % HBF_4/Et_2O solution.[15]

Of particular significance is that **1** may be also prepared from the structurally analogous 23-atom homopalladium species $Pd_{23}(CO)_{20}(PEt_3)_8$ (**3**).[4] The reaction sequence (2) is similar to that applied for the precursor **4**, except for the use of THF instead of acetone, in which cluster **3** is insoluble. Because **3** possesses an interstitial Pd atom, its transformations into the Au-encapsulated one can only have occurred by a combined fragmentation and reassembling process.

$$Pd_{23}(CO)_{20}(PEt_3)_8\ (\mathbf{3}) \xrightarrow[\text{b) } Au(SMe_2)Cl,\ 50\,^\circ C,\ 2\,h]{\text{a) } CF_3CO_2H/Me_3NO,\ 50\,^\circ C,\ 30\,min} [AuPd_{22}(CO)_{20}(PEt_3)_8][(CF_3CO_2)_2H]\ (\mathbf{1}) \quad (2)$$

Despite the exact ligand match in **3** and **1** (namely, 20 CO and 8 PEt_3), exclusion of the seemingly unnecessary deligation reagent, Me_3NO, from the first stage (a) did not increase the yield of **1** (ca. 25 %). Observation of the Pd^{II} complex, $(PEt_3)_2PdCl_2$, as one of the products of the reaction sequence (2) indicates that Pd^0 may have been oxidized by H^+[13b] and probably by Au^I as well.[2c]

The solid-state and solution IR spectra of **1**, **1a**, and **2** are in accordance with the presence of doubly and triply bridging CO groups. Both $^{31}P\{^1H\}$ and ^1H NMR spectra of these clusters, regardless of solvent used, indicate the retention of their solid-state cationic structures in solution in displaying equivalent intensities for the four P(D) and four P(E) ligands. The $^{31}P\{^1H\}$ NMR data for **1**, **1a**, and **2** as well as for the neutral species $(\mu_{14}\text{-Pd})Pd_{22}(CO)_{20}(PEt_3)_8$ (**3**) are given in Table 1. The two equivalent doublets in the $^{31}P\{^1H\}$ NMR spectrum of **2** (in [D$_6$]acetone solution) at $\delta_1 = 20.8$ ppm ($^3J_{P\text{-}Ag} = 3.2$ Hz) and $\delta_2 = 16.6$ ppm ($^3J_{P\text{-}Ag} = 17.5$ Hz) substantiate without doubt the encapsulation of the Ag atom. The observed couplings originate from the two ^{107}Ag and ^{109}Ag isotopes (each with a nuclear spin of $I = 1/2$ and natural

Table 1: $^{31}P\{^1H\}$ NMR data[a] for **1**, **1a**, **2**, and **3** with the isostructural $[(\mu_{14}\text{-}M)Pd_{22}]^z$ metal cores, M = Au (**1**,**1a**; $z=1+$), Ag (**2**; $z=1+$) and Pd (**3**; $z=0$).

Cluster	Chemical shifts, ppm[b] (multiplicity, assignment, $J_{P\text{-}X}$ Hz)[c]	Solvent
$[AuPd_{22}(CO)_{20}(PEt_3)_8]^+$	$\delta_1=22.5$ (s, 4P(D)), $\delta_2=17.4$ (s, 4P(E))	[D$_6$]acetone
as $[(CF_3CO_2)_2H]^-$ salt (**1**)	$\delta_1=22.5$ (s, 4P(D)), $\delta_2=17.0$ (s, 4P(E))	[D$_8$]THF
	$\delta_1=16.9$ (s, 4P), $\delta_2=10.8$ (s, 4P(E))	[D$_1$]chloroform
$[AuPd_{22}(CO)_{20}(PEt_3)_8]^+$	$\delta_1=22.4$ (s, 4P(D)), $\delta_2=17.4$ (s, 4P(E)),	[D$_6$]acetone
as $[PF_6]^-$ salt (**1a**)	$\delta_3=-139.7$ (sep, PF_6^-, $^1J(P,F)=707$ Hz)	
$[AgPd_{22}(CO)_{20}(PEt_3)_8]^+$	$\delta_1=20.8$ (d, 4P(D), $^3J(P,Ag)=3.2$ Hz),	[D$_6$]acetone
as $[(CF_3CO_2)_2H]^-$ salt (**2**)	$\delta_2=16.6$ (d, 4P(E), $^3J(P,Ag)=17.5$ Hz)	
$Pd_{23}(CO)_{20}(PEt_3)_8$ (**3**)	$\delta_1=17.6$ (s, 4P(D)), $\delta_2=13.3$ (s, 4P(E))	[D$_8$]THF
	$\delta_1=14.3$ (s, 4P(D)), $\delta_2=9.6$ (s, 4P(E))	[D$_1$]chloroform

[a] Obtained at RT under N_2. [b] relative to external 85% H_3PO_4 in D_2O. [c] intensity ratio $\delta_1/\delta_2=1/1$.

abundances of 51.8% and 48.2%, respectively). Importantly, the $^{31}P\{^1H\}$ NMR solution spectrum of **2** also allows the reliable assignment of the two ^{31}P signals in both MPd_{22} cations (M = Au, Ag). The higher-field doublet signal at 16.6 ppm in **2**, which has an approximately five times stronger $^3J_{P\text{-}Ag}$ coupling than that for the doublet signal at 20.8 ppm, is assigned to the four P(E) phosphorus atoms attached to the tetracapped Pd(E) atoms. This unambiguous assignment is based upon each Pd(E) being coordinated to four palladium atoms (namely, 2Pd(A), Pd(B), Pd(C)) of the $AgPd_{14}$ kernel versus coordination to only two Pd(A) atoms for each wingtip Pd(D) atom and also being about 0.4 Å closer to the encapsulated Ag than each Pd(D) atom. Thus, the resulting coupling interaction of the P(E) atoms with the encapsulated Ag should be much stronger than that of the P(D) atoms. The latter P(D) nuclei in **2** give rise to the lower-field chemical shift of 20.8 ppm with a $^3J_{P\text{-}Ag}$ coupling of only 3.2 Hz. Accordingly, as Table 1 shows, the nearly identical lower-field $^{31}P\{^1H\}$ NMR singlet signals from **1** and **1a** (in [D$_6$]acetone and [D$_8$]THF) at 22 ppm, and likewise the lower-field singlet at 18 ppm in the $^{31}P\{^1H\}$ NMR spectra of **3** (in [D$_8$]THF), are also assigned to the wingtip P(D) atoms. Replacement of the encapsulated Pd^0 atom in $(\mu_{14}\text{-}Pd)Pd_{22}(CO)_{20}(PEt_3)_8$ (**3**) with the much more electronegative coinage metal ions, Au^+ and Ag^+, expectedly shifts the ^{31}P NMR signals to lower fields.

CO/PR_3-ligated zerovalent Pd_n clusters with $n>10$ are unstable under CO. Entry 1 in Table 2 shows that the formal isostructural substitution of two non-isovalent zerovalent Au^0 atoms in place of two non-adjacent zerovalent Pd^0 atoms in $Pd_{23}(CO)_{20}(PEt_3)_{10}$ (**5**) to give the structurally analogous $Au_2Pd_{21}(CO)_{20}(PEt_3)_{10}$ (**6**) definitely suppresses CO-induced decomposition of the resulting Au-Pd cluster. The difference in stability between **6** and **5** is particularly noticeable in the solid state; whereas **6** can be kept indefinitely under CO, **5** may decompose after a few minutes, releasing smoke.[16] This stabilization of the Au-Pd cluster was attributed to delocalization of the two Au 6s^1 valence electrons. As previously mentioned, both crystallographic data and DFT calculations indicate that the higher stability to CO of the neutral Au_2Pd_{28} cluster relative to its Pd_{30} homopalladium analogue may likewise be ascribed to electron delocalization of each Au 6s valence electron for the two adjacent interior Au atoms, for which the alternative formation of a "localized" electron-pair Au–Au bond is not observed. In sharp contrast, entry 2 in Table 2 reveals that the isostructural but electronically equivalent formal incorporation of Au^+ into the $(\mu_{14}\text{-}Pd)Pd_{22}(CO)_{20}(PEt_3)_8$ (**3**) to give the $[(\mu_{14}\text{-}Au)Pd_{22}(CO)_{20}(PEt_3)_8]^+$ cation (**1**) does not affect the reactivities of either **3** or **1** toward CO. Both **1** and **3** exhibited the same degree of decomposition (ca. 80%) upon exposure to CO (at 50 °C in THF solutions after 2 h).

Table 2: Comparative reactivities toward CO for pairs of the isostructural clusters $Pd_{23}(CO)_{20}(PEt_3)_{10}$ (**5**) versus $Au_2Pd_{21}(CO)_{20}(PEt_3)_{10}$ (**6**) and $Pd_{23}(CO)_{20}(PEt_3)_8$ (**3**) versus $[AuPd_{22}(CO)_{20}(PEt_3)_8]^+$ (**1**).[a]

Entry	Pair	*t* [h]	Intact [%]
1	$Pd_{23}(CO)_{20}(PEt_3)_{10}$ (**5**)	0.5	0
	$Au_2Pd_{21}(CO)_{20}(PEt_3)_{10}$ (**6**)	2.0	60
2	$(\mu_{14}\text{-}Pd)Pd_{22}(CO)_{20}(PEt_3)_8$ (**3**)	2.0	17
	$[(\mu_{14}\text{-}Au)Pd_{22}(CO)_{20}(PEt_3)_8]^+$ (**1**)	2.0	18

[a] Relative stabilities were estimated from $^{31}P\{^1H\}$ NMR spectra after completion of the reactions performed under CO at 50 °C in THF solutions.

Experimental details of syntheses and spectroscopic/crystallographic characterizations are given in Supporting Information. CCDC 927693 (**1**), 927694 (**1a**·0.5 Me_2CO), and 927695 (**2**) contain the supplementary crystallographic data for this paper. These data can be obtained free of charge from The Cambridge Crystallographic Data Centre via www.ccdc.cam.ac.uk/data_request/cif.

Future plans include electrochemical analyses of **1** and **2** and an attempted isolation and spectroscopic/crystallographic characterization of the protonated cationic cluster $[HPd_n(CO)_x(PEt_3)_y]^+$.

Received: March 8, 2013
Published online: June 17, 2013

Keywords: cluster compounds · gold · palladium · silver · synthesis design

[1] a) Y. Negishi, K. Igarashi, K. Munakata, W. Ohgake, K. Nobusada, *Chem. Commun.* **2012**, *48*, 660; b) D. I. Enache, J. K. Edwards, P. Landon, B. Solsona-Espriu, A. F. Carley, A. A. Herzing, M. Watanabe, C. J. Kiely, D. W. Knight, G. J. Hutchings, *Science* **2006**, *311*, 362; c) C.-W. Yang, K. Chanda, P.-H. Lin, Y.-N. Wang, C.-W. Liao, M. H. Huang, *J. Am. Chem. Soc.* **2011**, *133*,

19993, and references therein; d) N. Toshima, K. Kawashima, *Chem. Lett.* **2012**, *41*, 1171; e) X. Gu, Z.-H. Lu, H.-L. Jiang, T. Akita, Q. Xu, *J. Am. Chem. Soc.* **2011**, *133*, 11822.

[2] a) E. G. Mednikov, L. F. Dahl, *Philos. Trans. R. Soc. London Ser. A* **2010**, *368*, 1301; b) *The Cambridge Structural Database (CSD)*; c) E. G. Mednikov, S. A. Ivanov, L. F. Dahl, *Inorg. Chem.* **2011**, *50*, 11795.

[3] A ^{1}H NMR spectrum of C_6D_6 extract from the residue that was obtained after evaporation of the solution (upon completion of the first stage (a) of the reaction sequence (1)) revealed the upfield hydrido signal at −17.5 ppm along with the downfield signals at 14.5, 13.3, and 9.8 ppm.

[4] a) E. G. Mednikov, N. K. Eremenko, Yu. L. Slovokhotov, Yu. T. Struchkov, *Zh. Vses. Khim. O-va. im. D. I. Mendeleeva* **1987**, *32*, 101 [in Russian]; b) atomic coordinates were kindly supplied by Prof. Yuri Slovokhotov (M.V. Lomonosov Moscow State University, Moscow).

[5] a) A detailed neutron diffraction study of potassium hydrogen bis(trifluoroacetate) and its deuterium analogue led to the proposal of a "genuinely symmetrical hydrogen bond" with the hydrogen in a single potential energy well in accordance with spectroscopic measurements: b) A. L. Macdonald, J. C. Speakman, *J. Chem. Soc. Perkin Trans. 2* **1972**, 825; c) B. Gómez-Lor, G. Hennrich, B. Alonso, A. Monge, E. Gutierrez-Puebla, A. M. Echavarren, *Angew. Chem.* **2006**, *118*, 4603; *Angew. Chem. Int. Ed.* **2006**, *45*, 4491; d) S. M. Landge, E. Tkatchouk, D. Benítez, D. A. Lanfranchi, M. Elhabiri, W. A. Goddard III, I. Aprahamian, *J. Am. Chem. Soc.* **2011**, *133*, 9812; e) J. Pawlas, Y. Nakao, M. Kawatsura, J. F. Hartwig, *J. Am. Chem. Soc.* **2002**, *124*, 3669; f) E. V. Karpova, A. I. Boltalin, Yu. M. Korenev, E. Kemnitz, S. I. Troyanov, *Koord. Khim.* **2000**, *26*, 489. [*Coord. Chem. Russ.*]; g) J. R. Lomprey, J. P. Selegue, *Organometallics* **1993**, *12*, 616.

[6] a) The initial isolobal analogy stating that the proton is isolobal to LAu^+ (where L denotes a two-electron donor such as PR_3) was established from seminal articles by Hoffmann,[6b] Mingos and Evans,[6c] Lauher,[6d] and Stone.[6e] Their use of an auxiliary ligand L with Au^+ was primarily based upon the presumed experimental absence of stable complexes not containing naked surface Au^I atoms (that is, those without coordination to a donor L ligand). However, in a 2012 publication, Raubenheimer and Schmidbaur[6f] have pointed out that extensive utilization of new physical techniques (for example, mass spectrometry and photoelectron spectroscopy) combined with more sophisticated theoretical calculations of complex systems, especially in the gas phase, emphasize that the Au^I-attached auxiliary ligand L no longer plays a fundamental role. Therefore, they support the premise that the isolobal relationship should be reduced to H^+/Au^+ instead of H^+/LAu^+ analogies: b) R. Hoffmann, *Angew. Chem.* **1982**, *94*, 725; *Angew. Chem. Int. Ed. Engl.* **1982**, *21*, 711; c) D. G. Evans, D. M. P. Mingos, *J. Organomet. Chem.* **1982**, *232*, 171; d) J. W. Lauher, K. Wald, *J. Am. Chem. Soc.* **1981**, *103*, 7648; e) F. G. A. Stone, *Angew. Chem.* **1984**, *96*, 85; *Angew. Chem. Int. Ed. Engl.* **1984**, *23*, 89; f) H. G. Raubenheimer, H. Schmidbaur, *Organometallics* **2012**, *31*, 2507, and references therein.

[7] a) Recently it was also shown that the two earlier reported Au-Pd cluster cations, $[Au_2Pd_{14}(CO)_9(PMe_3)_{11}]^{+}$[7b] and $[AuPd_9(CO)_9(PPh_3)_6]^+$,[7c] with non-ligated (naked) surface Au^I atoms (that previously were violators of the experimentally established premise stated in Ref. [6]), were incorrectly formulated as Au_2Pd_{14} and $AuPd_9$ clusters and are in fact Tl^I-Pd clusters, $[Tl_2Pd_{14}(CO)_9(PMe_3)_{11}]^+$ and $[TlPd_9(CO)_9(PPh_3)_6]^+$.[7d] b) R. C. B. Copley, C. M. Hill, D. M. P. Mingos, *J. Cluster Sci.* **1995**, *6*, 71; c) C. Willocq, S. Hermans, M. Devillers, B. Tinant, *Z. Kristallogr.* **2008**, *223*, 495; d) E. G. Mednikov, L. F. Dahl, *Chem. Commun.* **2013**, *49*, 1085.

[8] a) Two Au-Pd clusters, the neutral $Au_2Pd_{21}(CO)_{20}(PR_3)_{10}$, R = Et, Me, and the monoanion $[AuPd_{22}(CO)_{20}(PPh_3)_4(PMe_3)_6]^-$, each with one centered Au atom, were prepared under basic conditions.[8b] $Au_2Pd_{21}(CO)_{20}(PEt_3)_{10}$ was used as a precursor for synthesis of clusters with the completely encapsulated Au atoms, $Au_2Pd_{28}(CO)_{26}(PEt_3)_{10}$[2c] and $Au_2Pd_{41}(CO)_{27}(PEt_3)_{15}$;[8c] Other known CO/$PR_3$-stabilized Au-Pd clusters with fully encapsulated gold atoms include $Au_4Pd_{28}(CO)_{22}(PMe_3)_{16}$[8d] and $Au_4Pd_{32}(CO)_{28}(PMe_3)_{14}$;[8e] b) N. T. Tran, D. R. Powell, L. F. Dahl, *Dalton Trans.* **2004**, 209; c) N. T. Tran, D. R. Powell, L. F. Dahl, *Dalton Trans.* **2004**, 217; d) E. G. Mednikov, N. T. Tran, N. L. Aschbrenner, L. F. Dahl, *J. Cluster Sci.* **2007**, *18*, 253; e) E. G. Mednikov, L. F. Dahl, *J. Cluster Sci.* **2005**, *16*, 287.

[9] a) A. D. Burrows, D. M. P. Mingos, *Coord. Chem. Rev.* **1996**, *154*, 19; b) P. Braunstein, J. Rose, *Gold Bull.* **1985**, *18*, 17.

[10] a) M. F. Hallam, D. M. P. Mingos, T. Adatia, M. McPartlin, *J. Chem. Soc. Dalton Trans.* **1988**, 335; b) A. Albinati, K.-H. Dahmen, A. Togni, L. M. Venanzi, *Angew. Chem.* **1985**, *97*, 760; *Angew. Chem. Int. Ed. Engl.* **1985**, *24*, 766.

[11] N. C. Payne, R. Ramachandran, G. Schoettel, J. J. Vittal, R. J. Puddephatt, *Inorg. Chem.* **1991**, *30*, 4048.

[12] a) At room temperature, reactions of $Pd_{10}(CO)_{12}(PEt_3)_6$, with CF_3CO_2H and Me_3NO afford the neutral clusters, $Pd_{16}(CO)_{13}(PEt_3)_9$,[12b] $Pd_{23}(CO)_{20}(PEt_3)_{10}$,[12b,c] $Pd_{23}(CO)_{20}(PEt_3)_8$,[12b] $Pd_{34}(CO)_{24}(PEt_3)_{12}$,[12b] $Pd_{38}(CO)_{28}(PEt_3)_{12}$,[12b] $Pd_{66}(CO)_{46}(PEt_3)_{16}$;[12d] b) E. G. Mednikov, N. I. Kanteeva, *Izv. Akad. Nauk Ser. Khim.* **1995**, 167. [*Russ. Chem. Bull. (Engl. Trans.)* **1995**, *44*, 163]; c) E. G. Mednikov, J. Wittayakun, L. F. Dahl, *J. Cluster Sci.* **2005**, *16*, 429; d) E. G. Mednikov, S. A. Ivanov, I. V. Slovokhotova, L. F. Dahl, *Angew. Chem.* **2005**, *117*, 7008; *Angew. Chem. Int. Ed.* **2005**, *44*, 6848.

[13] a) G. J. Kubas, *Chem. Rev.* **2007**, *107*, 4152; b) V. V. Grushin, *Chem. Rev.* **1996**, *96*, 2011; c) C. Cugnet, D. Lucas, E. Collange, B. Hanquet, A. Vallat, Y. Mugnier, A. Soldera, P. D. Harvey, *Chem. Eur. J.* **2007**, *13*, 5338.

[14] V. N. Zudin, V. D. Chinakov, V. M. Nekipelov, V. A. Likholobov, Yu. I. Yermakov, *J. Organomet. Chem.* **1985**, *289*, 425.

[15] K.-H. Dahmen, D. Imhof, L. M. Venanzi, *Helv. Chim. Acta* **1994**, *77*, 1029.

[16] In particular, such an effect was observed for the finely crystalline samples and may have been induced by the presence of traces of coordinatively unsaturated Pd nanoparticles/colloidal particles commonly known as Pd black.

